Functionalized MoS_2/polyurethane sponge: An efficient scavenger for oil in water

Tianlong Yu[a,b], Dolci Mathias[b], Shixiang Lu[a], Wenguo Xu[a], Mu. Naushad[c,d], Sabine Szunerits[b] and Rabah Boukherroub[b,*]

[a] *School of Chemistry and Chemical Engineering, Beijing Institute of Technology, Beijing 100081, PR China*

[b] *Univ. Lille, CNRS, Centrale Lille, ISEN, Univ. Valenciennes, UMR 8520 – IEMN, F-59000 Lille, France*

[c] *Advanced Materials Research Chair, Department of Chemistry, College of Science, Bld#5, King Saud University, Riyadh, 11451, Saudi Arabia*

[d] *Department of Chemistry, College of Science, Bld#5, King Saud University, Riyadh, 11451, Saudi Arabia*

*To whom correspondence should be sent to: rabah.boukherroub@univ-lille.fr (+333 62 53 17 24)

Abstract

Advanced materials with special wettability hold promise in environmental remediation, catalysis or superfluid, and have attracted a great deal of interest in the last years. Herein, a composite material consisting of molybdenum sulfide/polyurethane sponge (MoS_2/PU) was fabricated through MoS_2 nanosheets loading onto PU using high-intensity sonication and subsequent chemical functionalization by *in-situ* generated diazonium salts. The MoS_2 enhanced the hydrophobicity and roughness of the PU sponge and its surface could be effectively modified with aryl and carbon-fluorine groups through diazonium chemistry. The resulting F-MoS_2/PU sample exhibited exceptional superhydrophobic/superoleophilic wettability, which provides the potential to separate oil/water mixtures or eliminate selectively oil from underwater or emulsions. Besides, due to the cavitation effect of high-intensity ultrasound, the exfoliated MoS_2 sheets were strongly anchored onto the PU sponge. Loading MoS_2 and/or diazonium molecules did not induce any adverse effect on the adsorption capacity of the sponge with values ranging from 25 to 90 gg^{-1} for different organic solvents (hexane, diethyl ether, ethanol, toluene, rapeseed oil, acetonitrile, dichloromethane and chloroform). Additionally, the hydrophobic groups covalently bonded to the surface conferred excellent stability to the MoS_2/PU material during repeated cycles of oil/water separation, or upon exposure to harsh environments (-20 or +120 ºC, acid solution of pH=1 and base solution of pH=14, NaCl solution of 3.0%, natural seawater, ethanol and chloroform).

Keywords: *PU sponge; molybdenum sulfide; in-situ diazonium salts; superhydrophobic/superoleophilic; stability.*

1. Introduction

Functionalized materials with amazing properties bring out inspiration to promote efficiency or overcome thorny issues encountered in the environment. The spill oil covers a large proportion of water contamination, especially that is caused by the leakage of organic reagents or unlawful discharging chemical wastes [1]. Their bio-toxicity brings disastrous effect to the aqueous system and dramatically cuts down the disposing efficiency in normal municipal treatment. For such cases, the efficient separation of oil from water by extracting the organic phase represents a promising approach for environment remediation or recyclable uses [2, 3]. For such applications, materials with distinctive water-repellency and oil-affinity hold great potential [4].

Numerous reports described the preparation of efficient materials with desired wettability for oil/water separation [5-7]. Theoretically, such materials normally exhibit an ideal surface roughness as well as appropriate surface energy, which is just lower than that of water and still higher than that of organics. Therefore, the water could be remarkably repelled, and meanwhile, the surface could be wetted by the majority of organics. Thus, the separation of oil and water phases can be easily achieved. For building such materials, several approaches including chemical or physical vapor deposition, electrochemical growth, spray coating, hydrothermal, solution immersion or sol-gel [8-11] have been proposed using different substrates such as glass, polymers, metals, alloys as well as fibers and textiles [12, 13]. A suitable combination of such method and substrate along with the modification of surface energy and morphology are two key parameters for achieving superhydrophobicity [14, 15].

Molybdenum disulfide (MoS_2), a family member of transition metal dichalcogenides, has

similar layer structure as graphene and also exhibits good chemical stability, enhanced electrical conductivity, rich surface chemistry, and hydrophobic properties. As such, it has been widely applied in wear-resistant, lubricating, supercapacitors, catalysis, etc. [16-19]. In addition, MoS_2 displays a hydrophobic character, which holds potential for developing MoS_2-based hydrophobic materials. Wan et al. [20] and Gao et al. [21] prepared hydrophobic MoS_2-coated melamine/formaldehyde sponge through a repeated dipping-drying process. Tang et al. [22] fabricated PU/MoS_2 nanocomposite coatings *via* implantation of MoS_2-PU/acetone on the surface of stainless steel, glass, paper and fabric substrates, followed by modification with perfluorooctyltrichlorosilane. However, these approaches usually require several coating/drying cycles (3-6 times) to ensure an efficient loading of MoS_2, resulting in reduced adsorption capacity. Furthermore, the deposited MoS_2 layers were not firmly attached to the surface, resulting in low stability [23]. This problem of coating stability can be addressed by using intensive sonication. Due to the cavitation effect of high-intensity ultrasonic irradiation, MoS_2 powder could be exfoliated into sheets and deposited onto the substrate by the countless micro-jets [24, 25]. Meanwhile, the local temperature of the micro-jet shocked area could be extremely high, as a result, the surface would be possibly burned and even melted and the delivered MoS_2 could be firmly embedded onto the substrate [26-28].

Moreover, for further improving the wettability of MoS_2-coated PU surface, the diazonium chemistry modification could be an ideal candidate [29]. In fact, diazonium salts have proven to be of high importance in organic synthesis and surface functionalization [30, 31]. Using diazonium salts, functional groups could be grafted onto the target surface *via* covalent bonds, which confers superior stability and reliability, compared to physical

adsorption or adhesive coating. A few reports revealed that MoS_2 could be modified by diazonium salts. Benson et al. [32] tailored the electronic property of MoS_2 through diazonium functionalization to achieve a balance between the catalytic property and stability. In their study on MoS_2 functionalization with diazonium salts, Knirsch et al. [33] proposed covalent bonding mechanism. Even though MoS_2 derivatization through diazonium chemistry has been described, application of the modified MoS_2 for oil/water separation remains scarce. In addition, the classic diazonium chemistry method, consisting in the preparation of diazonium salt and then perform modification, exhibits some limitations such as low-efficiency, complicated procedure, and the as-prepared salts are prone to decomposition. So, *in-situ* generated diazonium modification is applied to overcome these drawbacks. Indeed, such an approach is facile, effort-saving and promising for large scale.

Herein, a polyurethane (PU) sponge was selected as the substrate owing to its advantages like low cost, availability, ideal porosity, mechanical strength and chemical inertness. MoS_2-coated PU sponge was prepared *via* high-intensity sonication and further modification with *in-situ* generated aromatic diazonium salts. The optimum conditions were systematically investigated through water contact angle (WCA) measurements. Several oil/water mixtures were examined for testing its separation ability. Moreover, its reusability as well as stability in harsh environments were also studied. The results indicated that the functionalized sample has ideal superwettability as well as stability, which holds potential for separation. More importantly, the proposed method combining ultrasonication and diazonium modification is not only limited for MoS_2-PU sponge, but can be easily extended to other materials for various applications.

2. Experimental

2.1 Preparation of diazonium functionalized MoS_2 coated PU sponge (F-MoS_2-PU)

The F-MoS_2-PU sponge was prepared by MoS_2 coating and further covalent modification by *in-situ* generated diazonium salts. Initially, a PU sponge (~ 14 mg, 1×2 cm) was cleaned sequentially with ethanol and water under continuous sonication for 1 h each to remove surface contaminants. The clean sponge was annealed at 60 ^{o}C overnight to remove residual moisture. MoS_2 powder was dispersed in ethanol under sonication (5 min) and a clean PU sponge was added into the MoS_2 dispersion (2 mg/mL) and subjected to discontinuous high-intensity sonication (BRANSON 450 Digital Sonifier, 400 W at 50% efficiency, 2 s sonication and 1 s interval) for 30 min. The resulting MoS_2-coated PU sponge was rinsed with ethanol and dried at 60 ^{o}C for 1 h. Then the MoS_2-loaded PU sponge was immersed into a 5 mM solution of either aniline, 3,5-bis(trifluoromethyl) aniline or 4-(heptadecafluorooctyl) aniline in acetonitrile and 15 mM *tert*-butyl nitrite for 24 h. The formed F-MoS_2-PU sponge was cleaned with a copious amount of water, and dried in air.

3. Results and discussion

3.1. Preparation of superhydrophobic/superoleophilic (F-MoS_2-PU) sponge

The superhydrophobic/superoleophilic functionalized MoS_2-coated polyurethane (F-MoS_2-PU) sponge was prepared in a two-step process, as depicted in **Figure 1.** The first step consisted in coating the PU sponge with MoS_2 through a simple immersion of the PU sponge into an ethanolic solution of MoS_2 under high-intensity sonication to produce hydrophobic

MoS_2-PU composite. To achieve superhydrophobicity, the MoS_2-PU composite was subsequently *in-situ* functionalized with diazonium salts.

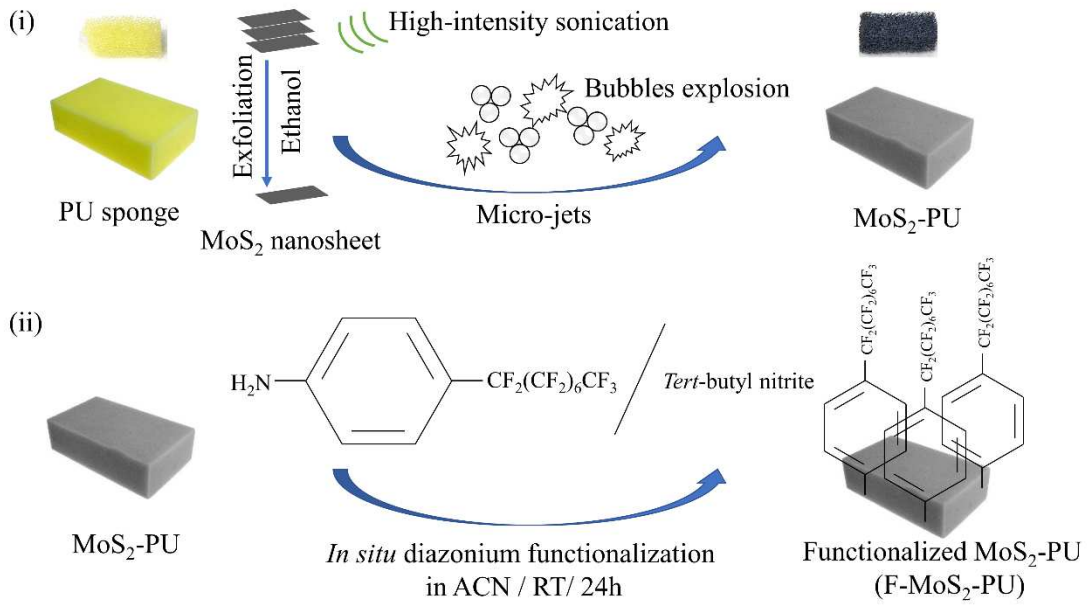

Figure 1: Schematic description of the preparation of a superhydrophobic/superoleophilic (F-MoS_2-PU) sponge using a two-step process: (i) coating PU sponge with MoS_2 to form MoS_2-PU followed by (ii) covalent modification with 4-(heptadecafluorooctyl) aniline through *in situ* generated diazonium salt.

During this process, the powerful ultrasound irradiation induced MoS_2 exfoliation into sheets and their subsequent coating onto the PU sponge *via* micro-jets, due to bubbles explosion owing to the cavitation effect [25]. In addition, the exfoliated MoS_2 sheets displayed excellent mechanical flexibility due to their effective interaction with the PU sponge through van der Waals forces [20]. An indirect evidence of the integration of MoS_2 nanosheets was the color change of the sponge from yellow to gray-black (**Figure 1**). The integration of hydrophobic heptadecafluorooctyl functional groups was based on the spontaneous reduction of diazonium salts *in situ* generated in acetonitrile in the presence of *tert*-butyl nitrite (*t*-BuONO). The

diazotization reaction assisted by *t*-BuONO produced diazonium moieties, which coupled spontaneously to the sulfur atoms of the two-dimensional MoS_2 nanosheets. In contrast to surface functionalization through physical coating, the covalent modification is reliable and contributes to enhanced stability of the coating.

3.2. Wetting properties

To assess the effect of MoS_2 coating and diazonium functionalization on the wetting properties of the PU sponge, static water contact angle (WCA) measurements were recorded. **Figure 2** indicates that the wettability of the bare PU sample exhibited an increasing trend upon functionalization with diazonium salts of 3,5-bis(trifluoromethyl) and 4-(heptadecafluorooctyl) anilines. In fact, the WCA of bare PU sponge increased from 95±1° to 115±1° and 125±1° upon incorporation of 3,5-bis(trifluoromethyl) and 4-(heptadecafluorooctyl)benzene moieties, respectively. Interestingly after MoS_2 coating, the WCA also increased from 95±1° (original state) to ~122±1°. Subsequent *in-situ* modification with diazonium salts of aniline, 3,5-bis (trifluoromethyl) aniline and 4-(heptadecafluorooctyl) aniline led to a steady increase of the WCA to 133±1°, 142±1° and 155±1°, respectively. The results indicate that superhydrophobicity was only achieved when the MoS_2-PU surface was functionalized with a long fluorinated (4-heptadecafluorooctyl) chain, contributing in reducing the surface energy of F-MoS_2-PU sponge.

For comparison, blank experiments were performed to highlight the influence of covalent modification *vs*. physical adsorption. In fact, when the MoS_2-PU sponge was immersed in the aniline precursor ethanolic solution in absence of *tert*-butyl nitrite, the MoS_2-PU sponge failed to reach superhydrophobicity. Although the WCA increased to 139±1° upon modification with

4-(heptadecafluorooctyl) aniline, its surface still exhibited obvious hysteresis; the water droplet remained stuck to the surface even when the sample was held perpendicularly. From the comparison, it could be concluded that the diazonium modification was necessary to reach superhydrophobicity.

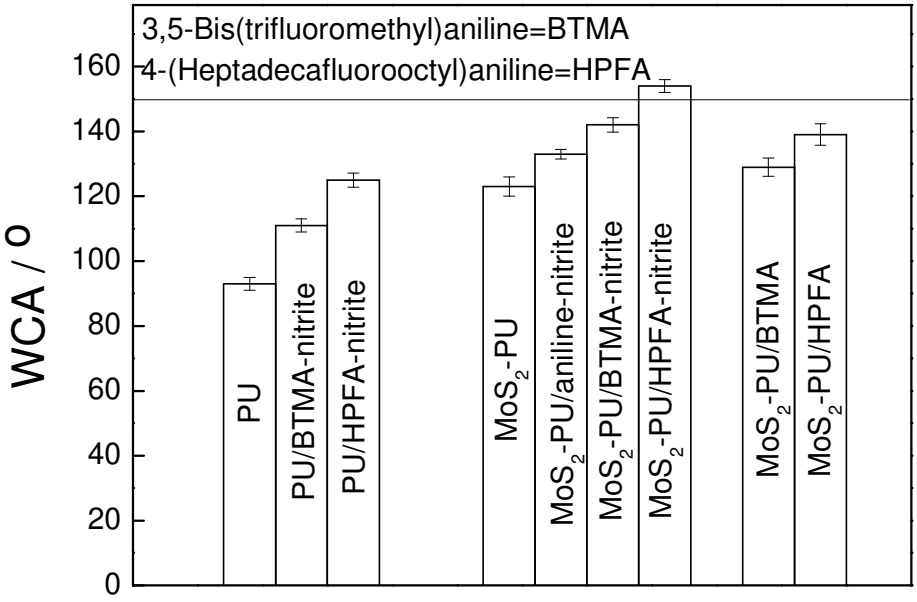

Figure 2: WCAs of bare PU and MoS_2-coated PU before and after functionalization with aniline, 3,5-bis(trifluoromethyl) aniline (BTMA), 4-(heptadecafluorooctyl) aniline (HPFA) diazonium salts. For comparison: MoS_2-PU was modified with BTMA and HPFA in absence of *tert*-butyl nitrite.

The results indicate that superhydrophobicity can be achieved upon functionalization with an aniline precursor bearing the longest fluorine chain *i.e.* 4-(heptadecafluorooctyl) aniline, which contributed in reducing the surface energy of the MoS_2-PU sponge and resulted in excellent wettability with a WCA over 150°. Therefore, the MoS_2 and *in-situ* generated diazonium salts collectively contributed to the excellent wettability, and the sample modified with 4-(heptadecafluorooctyl) aniline was used for the following study. Besides, the 4-(heptadecafluorooctyl) aniline functionalized MoS_2-PU (F-MoS_2-PU) surface could effectively

repel water; the droplets just roll down immediately once they contact the sample surface. This remarkable water-repelling property of F-MoS_2-PU was recorded in **supplementary video 1**.

The optical images of water droplets on bare PU, MoS_2-PU and F-MoS_2-PU sponges are summarized in **Figure 3**, exhibiting the change from a semi-sphere (bare PU, **Fig. 3a**) to an oval (MoS_2-PU, **Fig. 3b**) and a quasi-sphere (F-MoS_2-PU, **Fig. 3c**). A water droplet on F-MoS_2-PU stays above the twigs of the PU skeleton with a strong tendency to roll down. In fact, a water droplet could roll down from horizontally placed F-MoS_2-PU, indicating a low SWCA (< 5°). The successive snapshots of this rolling process were recorded in **Figure S1**.

In addition, the effects of extrusion cycles as well as abrasion on WCA and SWCA of F-MoS_2-PU were assessed using a 200 g load (**Figure S2**). Interestingly, under our experimental conditions, the WCA of the F-MoS_2-PU sample remained basically stable over ~150^o during 30 extrusion cycles with a negligible increase of the SWCA (**Fig. S2a**). Similarly, the WCA angle of the F-MoS_2-PU was not impacted by the abrasion test (**Fig. S2b**). In contrast, the SWCA increased steadily and reached a final value of ~ 18^o after 30 abrasion cycles (**Fig.S2b**). This phenomenon could be attributed to the partial damage of the surface structures. The results clearly revealed the good stability of F-MoS_2-PU, supporting its value for research and applications.

Actually, a water droplet dyed with methylene B was completely repelled from the F-MoS_2-PU surface, while a chloroform droplet dyed with rhodamine B completely wets the F-MoS_2-PU surface instantly due to the superhydrophobic/superoleophilic character of the sponge (**Fig. 3d**).

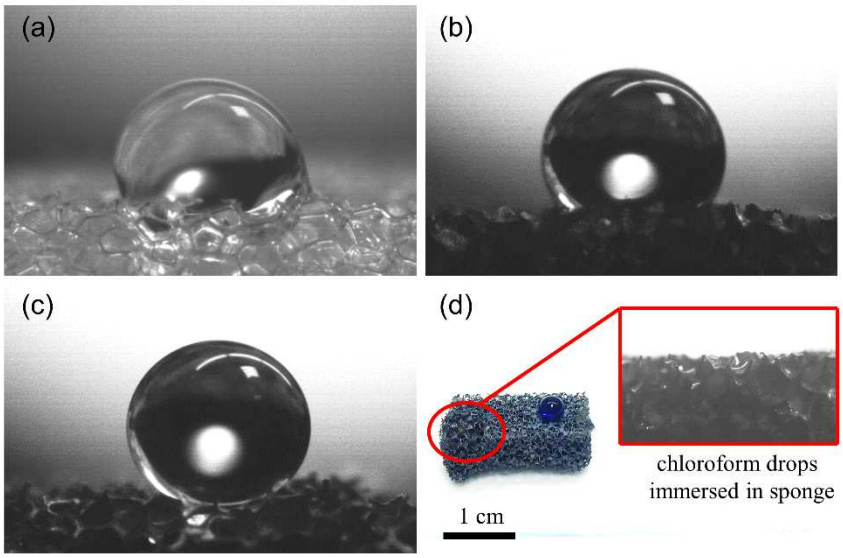

Figure 3: Optical images of water droplets on (a) bare PU sponge, (b) MoS_2-PU, (c) 4-(heptadecafluorooctyl) aniline functionalized MoS_2-PU (F-MoS_2-PU) and (d) illustration of the superhydrophobic/superoleophilic wettability; the inset is an optical image of a chloroform droplet on F-MoS_2-PU; the water is dyed with methylene blue and the chloroform droplet is dyed with rhodamine B for comparison. The dynamic process is available in **supplementary video 2**.

The inset in **Fig. 3d** reveals that chloroform has a contact angle of about 0°. This dynamic process is presented in **supplementary video 2**. The sample F-MoS_2-PU with distinguished wettability towards water and oil could be reckoned as a good separation membrane for oil/water mixtures.

Figure 4 depicts the surface morphology of the PU sample before and after MoS_2 coating and chemical functionalization with the diazonium salt of 4-(heptadecafluorooctyl) aniline. While the bare PU sponge displayed a relatively smooth surface morphology before and after high-intensity sonication, obvious changes can be evidenced after coating with MoS_2, as shown in **Figure S3**. Indeed, the MoS_2-PU sponge was covered by densely packed interconnected

MoS_2 nanoplatelets of irregular dimensions with an overall increase in surface roughness (**Fig. 4c-d**). This morphology most likely arises from the exfoliated MoS_2 sheets, immobilized on the PU sponge by the powerful micro-jets; some of the MoS_2 sheets are held together through van der Waals forces. As a result, these intertwined slices significantly switched the surface morphology, imparting the necessary roughness to enhance the hydrophobicity of the surface. These special blade-like structures maintained well during the *in-situ* generated diazonium salt modification step. The sample surface was still covered by countless flakes, stacking together by random layers (**Fig. 4e-f, Figure S4**). Nevertheless, the wettability of the resulting surface was altered upon diazonium modification with a significant increase of the WCA.

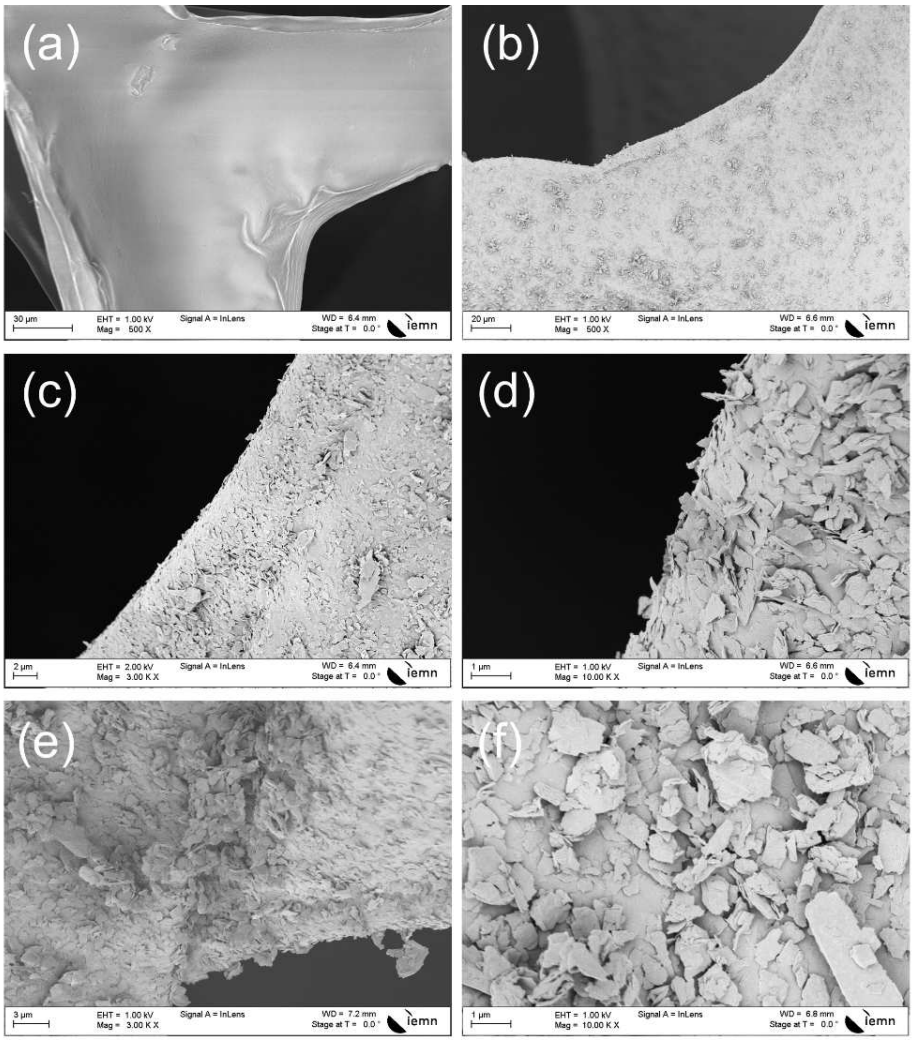

Figure 4: SEM images of (a) bare PU at ×500, (b-d) MoS_2-PU at different magnifications (×500, ×3k, ×10k) and (e-f) F-MoS_2-PU at ×3k and ×10k magnifications.

Additional characterizations were carried out for investigating the difference of chemical environment on F-MoS_2-PU surface. To get a clear picture on the chemical composition of F-MoS_2-PU sponge, XPS analysis was performed. **Figure 5** depicts the XPS spectra of the bare PU sponge (spectrum A) and F-MoS_2-PU sample (spectrum B). Accordingly, in **Fig. 5a**, the full survey spectrum of bare PU sponge comprises bands due to C 1s (~ 284 eV), N 1s (~ 398 eV), and O 1s (~ 530 eV). This is in full accordance with the elemental composition of the PU sponge. After coating with MoS_2 and subsequent functionalization with 4-(heptadecafluorooctyl) aniline, new peaks due to Mo 3d (~ 230 eV), S 2p (~ 162 eV), and F 1s (~ 688 eV) were detected on the spectrum B, originating from MoS_2 sheets and grafted diazonium molecules.

Figure S5a depicts the XPS high resolution spectrum of F 1s, comprising a strong fluorine signal at 688 eV from the carbon-fluorine groups in 4-(heptadecafluorooctyl) aniline moieties. Moreover, the change could be observed in the high-resolution spectrum of C 1s (**Fig.S5b**). There are obvious peaks at 284.4 and 288.1 eV, ascribed to C=C/C-C and C=O bonds, respectively. Notably, after chemical modification, additional contributions at higher binding energy attributed to -CF_2 (291.4 eV) and -CF_3 (293.3 eV) groups were observed on the spectrum B (**Fig.5b**) [31, 34]. Therefore, it could be concluded that the PU surface was successfully modified by the *in-situ* generated diazonium salts. In addition, as illustrated in **Figure S5c**, the peaks located at 228.6 eV (Mo 3d5/2) and 231.8 eV (Mo 3d3/2) with a separation of 3.2 eV agrees well with the value of 3.14 eV of MoS_2 [18].

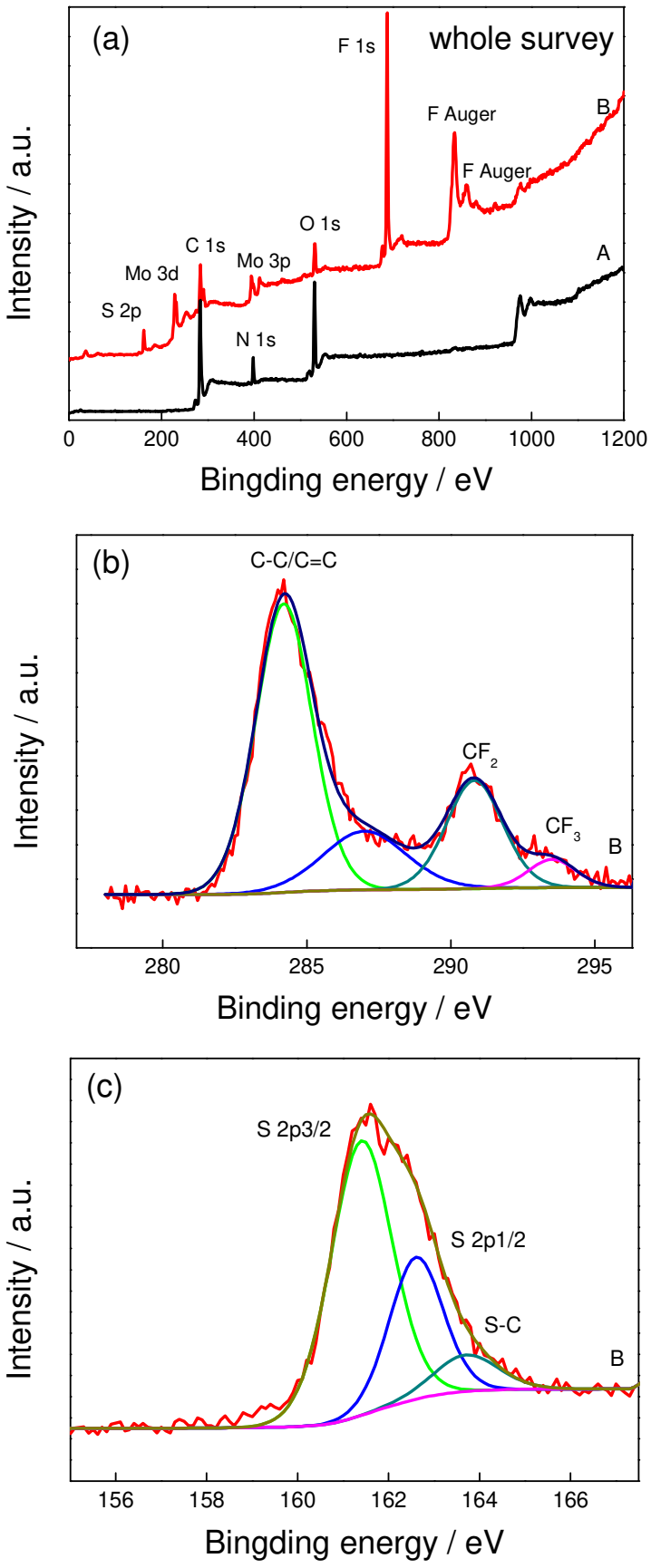

Figure 5: (a) XPS full survey spectra of bare PU sponge (spectrum A) and F-MoS_2-PU

sponge (spectrum B), (b) fitted curves of spectrum B of C 1s and (c) S 2p.

Meanwhile, the XPS high resolution spectrum of S 2p could be deconvoluted into two peaks centered at 161.4 eV (S $2p_{3/2}$) and 162.6 eV (S $2p_{1/2}$) with a separation of 1.2 eV, as expected for MoS_2 (**Fig. 5c**). Moreover, an additional feature at ~163.7 eV **(Fig.5c)** is consistent with the binding energy of S-C bond, which provides the evidence that the modification of MoS_2 layer by diazonium chemistry *via* covalent bonds. Therefore, these results indicate that the PU sponge was coated by MoS_2 and 4-(heptadecafluorooctyl) aniline moieties.

Figure 6 illustrates the ATR-FITR spectra of PU and F-MoS_2-PU sponge samples in the 600 to 1800 cm^{-1} frequency range. For the bare PU sponge (spectrum A), the peaks located at 3296 and 2961 cm^{-1} are ascribed to the stretching vibrations of N-H and C-H, respectively **(Figure S6)**. Additionally, the peaks at 1730 and 1641 cm^{-1} are respectively assigned to C=O stretching in ester and urea groups, and the peak at 1536 cm^{-1} is due to the amide II band stretching [35]. Additional bands at 1222 and 1182 cm^{-1} are associated with O-C-O stretching in ester and at 1130 cm^{-1} is attributed to C-O stretching in ether group. For the F-MoS_2-PU (spectrum B), there are new peaks at 1147 and 1203 cm^{-1}, corresponding to the C-F bonds, which are attributed to CF_2 and CF_3 groups in the diazonium layer. Although there are some interferences from other peaks in this area, the new C-F peaks still could be distinguished apart, as illustrated in the inset. Also, a medium intensity but obvious peak at 705 cm^{-1} offers a substantial evidence for the formation of S-C bond [33] and consistent with the XPS results, as the result of successful diazonium modification.

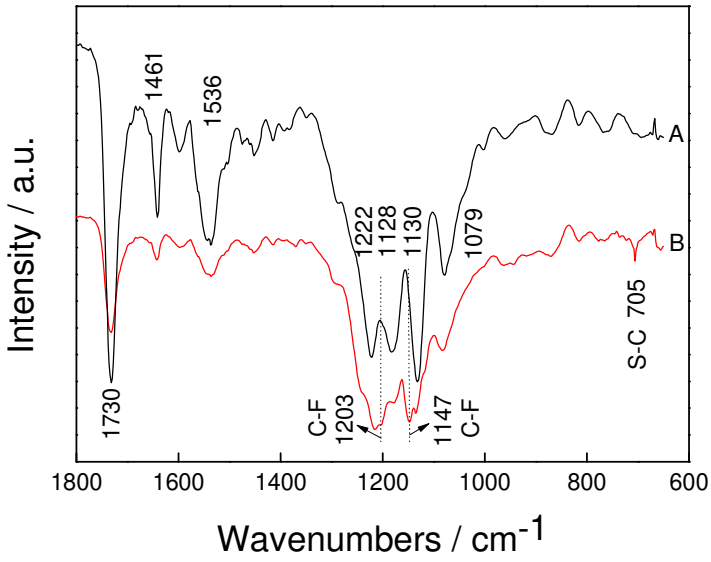

Figure 6: ATR-FTIR spectra of bare PU sponge (spectrum A, black) and F-MoS_2-PU sponge (spectrum B, red).

In addition, it is worthy to mention that after the ATR-FTIR characterization, the sample was pressed into a quite thin slice by the detecting pole. However, it could gradually restore the original shape and maintain the same wettability, which indicates ideal mechanical durability.

3.2 Stability

Figure 7 summarizes the results of the stability studies of the F-MoS_2-PU in harsh environments including pH (1 and 14), corrosive 3% NaCl aqueous solution as well as different temperatures (-20 or +120 ^{o}C). No apparent change of the WCA was observed upon exposure of the F-MoS_2-PU to these conditions. Similarly, the wettability of the F-MoS_2-PU sample was not altered upon immersion in natural seawater for 3 days. In addition, the sample was also immersed in ethanol and chloroform for 24 h, for testing the resistance towards the dissolution in organic solvents. It turned out that the sample still holds desired wettability in general with an apparent WCA of ~150^{o}. However, for the sample immersed in chloroform, its roll-down property faded and a few particles detachment could be observed when the sample was washed

with ethanol. This was ascribed to the presence of loosely attached MoS_2 layers by van der Waals forces and the swelling-shrinking transformation of PU skeleton. Even though partial MoS_2 loss was unfavorable for water rolling down, it did not affect the surface apparent wettability so much and the WCA remained as high as ~ 150°. In addition, when the F-MoS_2-PU was placed at -20 or +120ºC, its wettability barely changed and also maintained excellent roll-down ability. For the sample placed in air atmosphere, the surface wettability was stable over 3 months. In general, owing to the chemical inertness of MoS_2 (immune to normal acid or base) and the covalent bonds built *via* diazonium modification, the F-MoS_2-PU holds ideal stability in such harsh conditions.

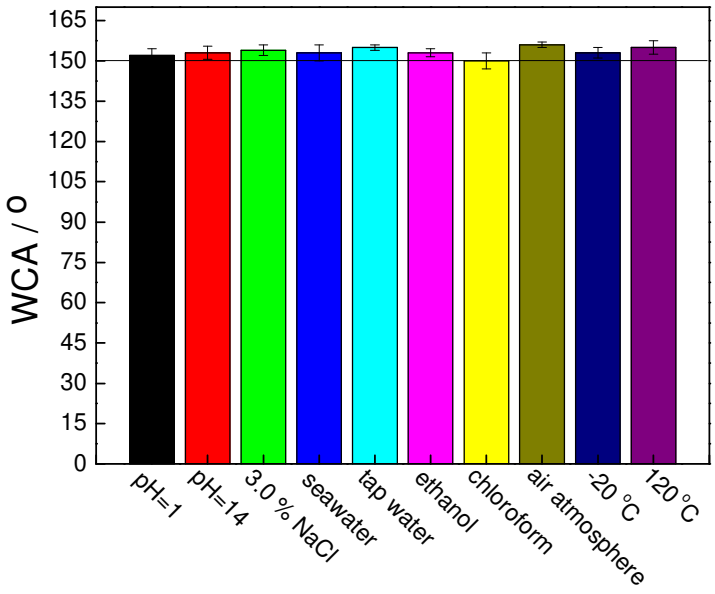

Figure 7: WCA of F-MoS_2-PU sponge placed in various conditions: immersed in pH=1, pH=14, 3.0% NaCl aqueous solution, tap water, ethanol and chloroform for 24 h, seawater for 72 h, air atmosphere for 3 months, at -20 ºC and +120 ºC for 1 h.

3.3 Oil adsorption

The oil adsorption capacity of F-MoS_2-PU was determined using equation (1):

$$C\ (gg^{-1}) = (m_i - m_o)/m_o \quad (1)$$

where m_i is the weight of the sponge after oil adsorption (g) and m_o is the weight of the original dry PU sponge (g).

From the results in **Figure 8a**, the adsorption capacity ranged from 25 to 90 gg^{-1} and followed an ascendant tendency with the increase of density in general. F-MoS_2-PU basically displayed a comparable adsorption capacity with that of bare PU sponge towards such organics. Additionally, for high density or viscosity organic solvents such as toluene, rapeseed oil, dichloromethane and chloroform, it exhibited even a better adsorption capacity.

Table 1. Adsorption capacity of different absorbents reported in the literature.

Material	Absorbed organics	Adsorption Capacity [k]	Ref.
F-MoS_2-PU sponge	hexane, diethyl ether, ethanol, toluene, rapeseed oil, acetonitrile, dichloromethane and chloroform	25-90	Present work
MoS_2-MF sponge	Chloroform, silicone oil, isopropanol, methylbenzene, edible oil, cyclohexane, gasoline	56-104	[23]
OTS-MF sponge	toluene, light petroleum, and methylsilicone oil	42-68	[36]
Spongy Graphene	Toluene, hexane, chloroform, pump oil, soybean oil, ethanol, DMSO, ethylbenzene,	20-86	[37]
NDs-PDA-PFDT-PU sponge	Chloroform, diesel, pump oil, gasoline, ethanol, toluene, hexadecane, hexane	4–60	[7]
Fe_3O_4@GO@OTS PU sponge	Lubricating oil, peanut oil, hexadecane, octane, hexane, heptane	9-27	[38]
CNT/PDMS-PU sponge	Soybean oil, used motor oil, diesel oil, n-hexadecane, gasoline, n-hexane	15-25	[39]

k refers to the times of the weight of adsorbed substances *vs.* the weight of adsorbent. PU: polyurethane; MF: melamine formaldehyde; OTS: octadecyltrichlorosilane; CNT: carbon nanotubes; NDs: nanodiamonds; PDA: polydopamine; PFDT: *1H,1H,2H,2H*-perfluorodecanethiol; GO: graphene oxide; PDMS: polydimethylsiloxane

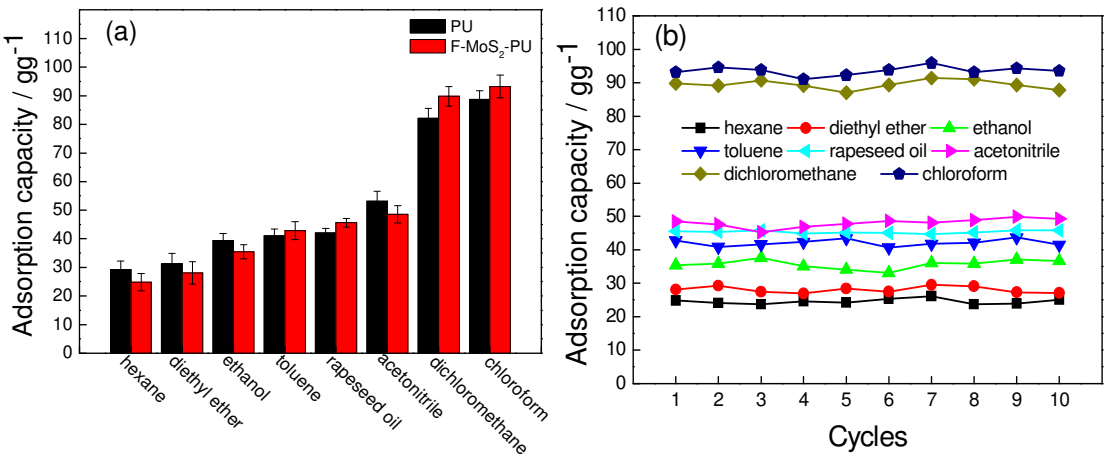

Figure 8: Oil adsorption capacity (**a**) and cycling stability (**b**) of F-MoS_2-PU towards different organic solvents (hexane: 0.69 g/mL, diethyl ether: 0.72 g/mL, ethanol: 0.79 g/mL, toluene: 0.87 g/mL, rapeseed oil: ~ 0.90 g/mL, acetonitrile: 0.79 g/mL, dichloromethane: 1.33 g/mL and chloroform: 1.48 g/mL).

Moreover, the F-MoS_2-PU revealed high stability in the adsorption/cleaning/drying/re-adsorption process. The results in **Figure 8b** and **Figure S7** indicated that the adsorption process was barely affected after 10 repeated cycles, indicating the high stability of F-MoS_2-PU. In addition, the adsorption capacity of F-MoS_2-PU was comparable to or better than that of the absorbing materials reported in the recent literature (**Table 1**).

3.4 Oil/water separation and elimination of local stained oil in water

To study the oil/water separation ability of F-MoS_2-PU, the separation of a chloroform/water mixture (7/3 volume ratio) where the organic phase was dyed with rhodamine B, is illustrated in **Figure 9**. When the chloroform (dyed with rhodamine B)/water mixture was poured into the funnel, the water phase accumulated above F-MoS_2-PU, while the pink chloroform crossed the F-MoS_2-PU membrane and dropped down to the bottle below the

funnel. The final collected chloroform volume was comparable to the initial one, indicating high separation efficiency (the whole separation process is available in **supplementary video 3**). The filtration was effective and facile, and F-MoS_2-PU was reused over 10 times without showing obvious deterioration of its separation efficiency (**Figure S8a**).

Additionally, the filtration flux was calculated using the following equation: Flux=V/At, where V (L) is the permeation volume, A (m^2) is the effective permeation area, and t (h) is the effective permeation time.

For the separation experiment, the F-MoS_2-PU sponge was compressed and fixed into the tunnel of a funnel. So the effective permeation area corresponds to the cross-sectional area of the funnel (Ø=5 mm). Consequently, the flux could be determined as ~5.35 $\times 10^3$ $Lm^{-2}h^{-1}$. This value remained stable during the cyclic separation processes (**Figure S8b**).

Moreover, for simulating partial oil contamination, a rhodamine B dyed chloroform droplet (~ 200 μL) was placed at the bottom of a beaker, which was filled with water. As depicted in **Figure 10**, the whole surface of F-MoS_2-PU was covered by an intact air layer with a silver-like color, demonstrating excellent superhydrophobic property.

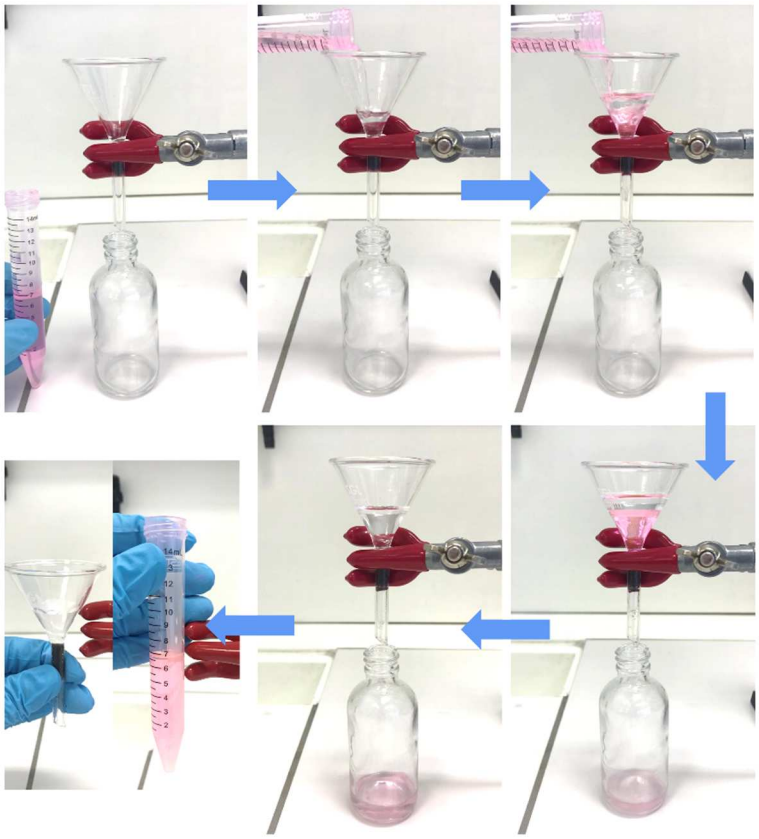

Figure 9: Oil water separation using F-MoS_2-PU: Photographs of the separation process of a chloroform/water (7/3 volume ratio) mixture using a home-made device; the chloroform is dyed with rhodamine B.

As the sample approaching the pink droplet, a mirror effect appeared, reflecting the pink color on the F-MoS_2-PU. Subsequently, once the sample contacted the droplet, the chloroform was absorbed by the F-MoS_2-PU sponge immediately. Meanwhile, the oil-loaded part became dark and an air bubble occurred at the bottom of F-MoS_2-PU, stemming from the absorbed chloroform pushing the air out of the F-MoS_2-PU skeleton. The rest part of the F-MoS_2-PU sponge was still occupied by air and displayed a silver-like color, indicating that the sample has potential of quenching larger amount of oil. At the end, when the sample was withdrawn from the beaker, the water restored its transparency with no pink trace (the whole separation process is available in **supplementary video 4**).

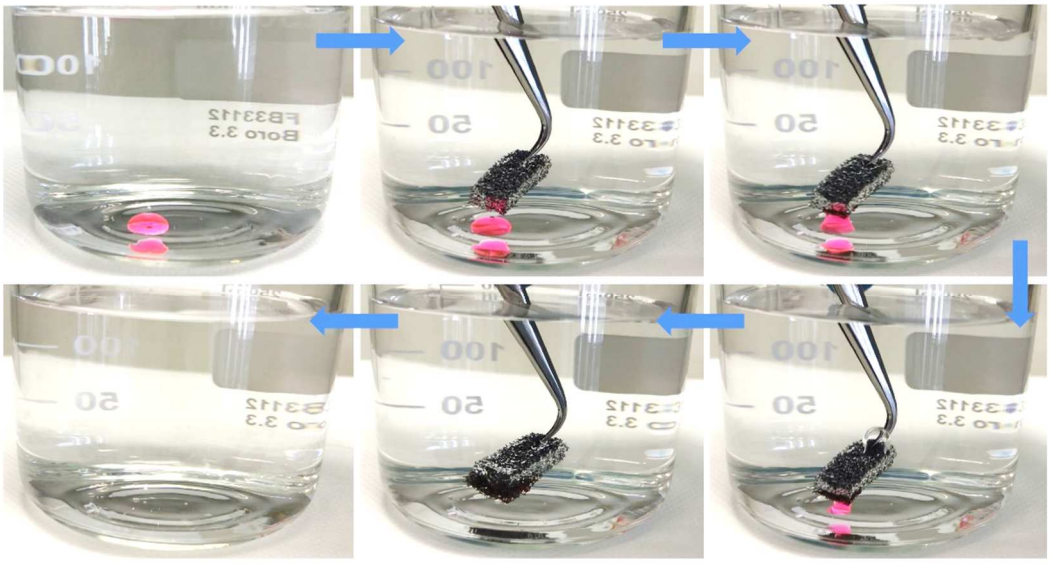

Figure 10: Snapshots of quenching of a chloroform droplet (~ 200 µL) underwater; the chloroform was dyed with rhodamine B.

3.5 Demulsification

A surfactant-stabilized toluene/water emulsion was prepared by adding Pluronic F-127 (0.1 mg/mL). The resulting emulsion was stable for 5 h, which was long enough for the demulsification process and characterization. The as-prepared F-MoS_2-PU was immersed into the emulsion and the color of the emulsion changed from milky to transparent, due to demulsification (**Figure 11a-b**, the whole process is available in **supplementary video 5**). The demulsified colorless solution was characterized by optical images and UV-vis spectrophotometry for determining the toluene content [40]. Owing to the superhydrophobic/superoleophilic property of F-MoS_2-PU, it was able to quench the emulsified oil in water even when the oil droplets size was around 5-20 µm (**Fig. 11c-d**). According to the calibration curve (see SI, **Fig. S9**), the content of remaining toluene was determined as ~0.16%, indicating a ~96.80% clearance. Moreover, the applied F-MoS_2-PU

holds repeated ability in demulsification as well. Accordingly, the F-MoS_2-PU was effective over 6 times with an average toluene removal over 96%.

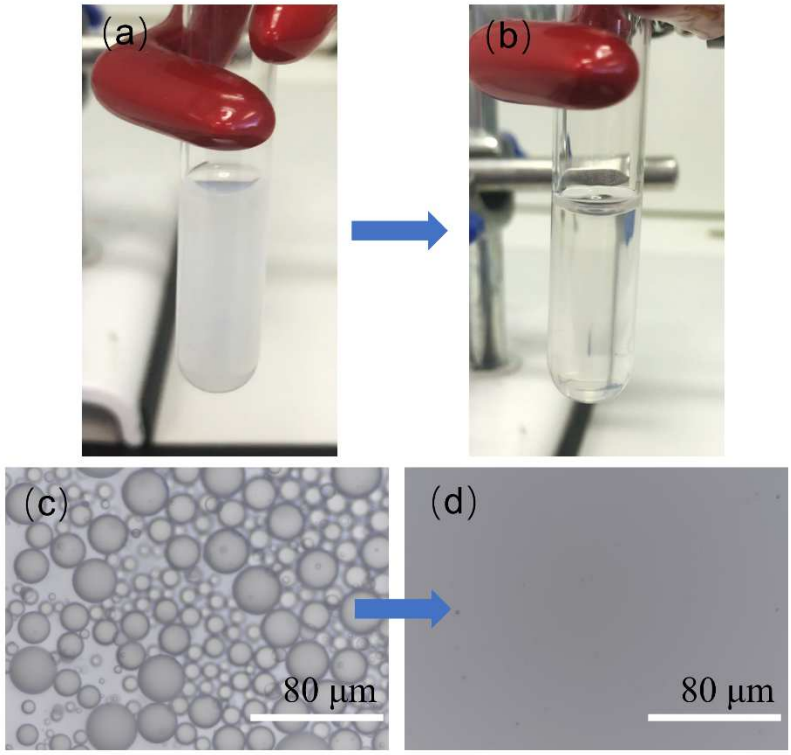

Figure 11: Snapshots of Pluronic F-127 stabilized toluene/water emulsion (5/95 volume ratio) before (a) and after (b) separation; Optical photographs of Pluronic F-127 stabilized toluene/water emulsion before (c) and after (d) separation.

4. Conclusion

An efficient MoS_2-coated polyurethane (PU) sponge was fabricated using an easy and simple approach, consisting of an extensive sonication coating followed by *in-situ* functionalization with diazonium salts. As a result, the exfoliated MoS_2 sheets adhered perfectly onto the PU sponge and were covalently modified with perfluoro groups. The resulting functionalized MoS_2-coated PU sponge (F-MoS_2-PU) displayed excellent wettability and was successfully applied for oil-water separation as well as selective elimination of oil

from underwater or demulsification of toluene/water mixtures. For the oil/water separation, the sample could be re-applied over 10 times without any apparent degradation of the separation efficiency. The work described in the present study provides an efficient, mild and promising method to fabricate functional super-wetting materials with remarkable stability using a facile process. It is worthy to notice that the proposed method could be applied for other applications such as corrosion resistance, bacterial elimination, catalysis or sensors, *via* applying different particles or substrates and diazonium salts for imparting desired groups. Actually, a work on functional bacterial killing materials is under investigation, and some promising results are obtained.

Supplementary files

The supplementary figures and videos are available in the supplementary information.

Acknowledgment

R.B., S.S. and T.Y. gratefully acknowledge financial support from the Centre National de Recherche Scientifique (CNRS), the University of Lille and the Hauts-de-France region. T.Y. gratefully thanks the Chinese government for the China Scholarship Council Award. S.L., W.X. and T.Y. gratefully acknowledge the National Natural Science Foundation of China (No. 21271027) for this work.

References

[1] H. Kang, Z. Cheng, H. Lai, H. Ma, Y. Liu, X. Mai, Y. Wang, Q. Shao, L. Xiang, X. Guo, Superlyophobic anti-corrosive and self-cleaning titania robust mesh membrane with enhanced oil/water separation, Sep. Purif. Technol. 201 (2018) 193-204.

[2] L. Wen, Y. Tian, L. Jiang, Bioinspired super-wettability from fundamental research to practical applications, Angew. Chem. Int. Ed. 54 (2015) 3387-3399.

[3] Y. Yang, X. Li, X. Zheng, Z. Chen, Q. Zhou, Y. Chen, 3D-Printed Biomimetic Super-Hydrophobic Structure for Microdroplet Manipulation and Oil/Water Separation, Adv. Mater. 30 (2018) 1704912.

[4] N. Chen, Q. Pan, Versatile fabrication of ultralight magnetic foams and application for oil-water separation, ACS Nano 7 (2013) 6875-6883.

[5] M. Khosravi, S. Azizian, Preparation of superhydrophobic and superoleophilic nanostructured layer on steel mesh for oil-water separation, Sep. Purif. Technol. 172 (2017) 366-373.

[6] W. Ma, Z. Guo, J. Zhao, Q. Yu, F. Wang, J. Han, H. Pan, J. Yao, Q. Zhang, S.K. Samal, Polyimide/cellulose acetate core/shell electrospun fibrous membranes for oil-water separation, Sep. Purif. Technol. 177 (2017) 71-85.

[7] N. Cao, B. Yang, A. Barras, S. Szunerits, R. Boukherroub, Polyurethane sponge functionalized with superhydrophobic nanodiamond particles for efficient oil/water separation, Chem. Eng. J. 307 (2017) 319-325.

[8] S. Ashoka, N. Saleema, D.K. Sarkar, Tuning of superhydrophobic to hydrophilic surface: A facile one step electrochemical approach, J. Alloys Compd. 695 (2017) 1528-1531.

[9] S. Amigoni, E. Taffin de Givenchy, M. Dufay, F. Guittard, Covalent layer-by-layer assembled superhydrophobic organic-inorganic hybrid films, Langmuir 25 (2009) 11073-11077.

[10] L.B. Boinovich, E.B. Modin, A.R. Sayfutdinova, K.A. Emelyanenko, A.L. Vasiliev, A.M.

Emelyanenko, Combination of Functional Nanoengineering and Nanosecond Laser Texturing for Design of Superhydrophobic Aluminum Alloy with Exceptional Mechanical and Chemical Properties, ACS Nano 11 (2017) 10113-10123.

[11] S.A. Mahadik, M.S. Kavale, S.K. Mukherjee, A.V. Rao, Transparent Superhydrophobic silica coatings on glass by sol–gel method, Appli. Surf. Sci. 257 (2010) 333-339.

[12] P.N. Manoudis, I. Karapanagiotis, A. Tsakalof, I. Zuburtikudis, C. Panayiotou, Superhydrophobic composite films produced on various substrates, Langmuir 24 (2008) 11225-11232.

[13] G. Ren, Y. Song, X. Li, Y. Zhou, Z. Zhang, X. Zhu, G. Ren, Y. Song, X. Li, Y. Zhou, A superhydrophobic copper mesh as an advanced platform for oil-water separation, Appl. Surf. Sci. 428 (2017).

[14] L. Feng, S. Li, Y. Li, H. Li, L. Zhang, J. Zhai, Y. Song, B. Liu, L. Jiang, D. Zhu, Super-hydrophobic surfaces: from natural to artificial, Adv. Mater. 14 (2002) 1857-1860.

[15] N. Cao, J. Guo, R. Boukherroub, Q. Shao, X. Zang, J. Li, X. Lin, H. Ju, E. Liu, C. Zhou, Robust superhydrophobic polyurethane sponge functionalized with perfluorinated graphene oxide for efficient immiscible oil/water mixture, stable emulsion separation and crude oil dehydration, Sci. China Technol. Sci. 62 (2019) 1585-1595.

[16] J. Choi, J. Mun, M.C. Wang, A. Ashraf, S.-W. Kang, S. Nam, Hierarchical, dual-scale structures of atomically thin MoS2 for tunable wetting, Nano lett., 17 (2017) 1756-1761.

[17] Y. Zhang, P. Ju, C. Zhao, X. Qian, In-situ grown of MoS_2/RGO/MoS_2@Mo nanocomposite and its supercapacitor performance, Electrochim. Acta 219 (2016) 693-700.

[18] G.R. Bhimanapati, T. Hankins, Y. Lei, R.A. Vilá, I. Fuller, M. Terrones, J.A. Robinson,

Growth and tunable surface wettability of vertical MoS_2 layers for improved hydrogen evolution reactions, ACS Appl. Mater. Interfaces 8 (2016) 22190-22195.

[19] P. Thangasamy, T. Partheeban, S. Sudanthiramoorthy, M. Sathish, Enhanced superhydrophobic performance of BN-MoS_2 heterostructure prepared via a rapid, one-pot supercritical fluid processing, Langmuir 33 (2017) 6159-6166.

[20] Z. Wan, Y. Jiao, X. Ouyang, L. Chang, X. Wang, Bifunctional MoS_2 coated melamine-formaldehyde sponges for efficient oil–water separation and water-soluble dye removal, Appl. Mater. Today 9 (2017) 551-559.

[21] X. Gao, X. Wang, X. Ouyang, C. Wen, Flexible Superhydrophobic and Superoleophilic MoS_2 sponge for highly efficient oil-water separation, Sci. Rep. 6 (2016) 27207.

[22] Y. Tang, J. Yang, L. Yin, B. Chen, H. Tang, C. Liu, C. Li, Fabrication of superhydrophobic polyurethane/MoS_2 nanocomposite coatings with wear-resistance, Colloids Surf. A 459 (2014) 261-266.

[23] Z. Wan, Y. Liu, S. Chen, K. Song, Y. Peng, N. Zhao, X. Ouyang, X. Wang, Facile fabrication of a highly durable and flexible MoS_2@RTV sponge for efficient oil-water separation, Colloids Surf. A 546 (2018) 237-243.

[24] S. Song, H. Yang, C. Su, Z. Jiang, Z. Lu, Ultrasonic-microwave assisted synthesis of stable reduced graphene oxide modified melamine foam with superhydrophobicity and high oil adsorption capacities, Chem. Eng. J. 306 (2016) 504-511.

[25] I. Perelshtein, G. Applerot, N. Perkas, J. Grinblat, E. Hulla, E. Wehrschuetz-Sigl, A. Hasmann, G. Guebitz, A. Gedanken, Ultrasound radiation as a “throwing stones” technique for the production of antibacterial nanocomposite textiles, ACS Appl. Mater. Interfaces 2 (2010)

1999-2004.

[26] V. Pol, H. Grisaru, A. Gedanken, Coating noble metal nanocrystals (Ag, Au, Pd, and Pt) on polystyrene spheres via ultrasound irradiation, Langmuir 21 (2005) 3635-3640.

[27] J. Gao, M. Hu, Y. Dong, R.K. Li, Graphite-nanoplatelet-decorated polymer nanofiber with improved thermal, electrical, and mechanical properties, ACS Appl. Mater. Interfaces 5 (2013) 7758-7764.

[28] I. Perelshtein, G. Applerot, N. Perkas, E. Wehrschetz-Sigl, A. Hasmann, G. Guebitz, A. Gedanken, Antibacterial properties of an in situ generated and simultaneously deposited nanocrystalline ZnO on fabrics, ACS Appl. Mater. Interfaces 1 (2008) 361-366.

[29] H. Li, C. Huang, L. Zhang, W. Lou, Fabrication of superhydrophobic surface on zinc substrate by 3-trifluoromethylbenzene diazonium tetrafluoroborate salts, Appl. Surf. Sci. 314 (2014) 906-909.

[30] Y.R. Thomas, A. Benayad, M. Schroder, A. Morin, J.l. Pauchet, New method for super hydrophobic treatment of gas diffusion layers for proton exchange membrane fuel cells using electrochemical reduction of diazonium salts, ACS Appl. Mater. Interfaces 7 (2015) 15068-15077.

[31] S. Gam, J. Pinson, P. Decorse, Y. Luo, R. Herbaut, L. Royon, C. Mangeney, Diazonium Salt Chemistry For The Design Of Nano-Textured Anti-Icing Surfaces, Chem. Commun. 54 (2018) 8983-8986.

[32] E.E. Benson, H. Zhang, S.A. Schuman, S.U. Nanayakkara, N.D. Bronstein, S. Ferrere, J.L. Blackburn, E.M. Miller, Balancing the hydrogen evolution reaction, surface energetics, and stability of metallic MoS_2 nanosheets via covalent functionalization, J. Am. Chem. Soc. 140

(2017) 441-450.

[33] K.C. Knirsch, N.C. Berner, H.C. Nerl, C.S. Cucinotta, Z. Gholamvand, N. McEvoy, Z. Wang, I. Abramovic, P. Vecera, M. Halik, Basal-plane functionalization of chemically exfoliated molybdenum disulfide by diazonium salts, ACS Nano 9 (2015) 6018-6030.

[34] Y. Cheng, G. He, A. Barras, Y. Coffinier, S. Lu, W. Xu, S. Szunerits, R. Boukherroub, One-step immersion for fabrication of superhydrophobic/superoleophilic carbon felts with fire resistance: fast separation and removal of oil from water, Chem. Eng. J. 331 (2018) 372-382.

[35] X. Zhang, F. Fu, X. Gao, X. Hou, Magnetically Driven Superhydrophobic Polyurethane Sponge for High Efficiency Oil/Water Mixtures Separation, J. Bionic Eng. 16 (2019) 38-46.

[36] Q. Ke, Y. Jin, P. Jiang, J. Yu, Oil/water separation performances of superhydrophobic and superoleophilic sponges, Langmuir 30 (2014) 13137-13142.

[37] H. Bi, X. Xie, K. Yin, Y. Zhou, S. Wan, L. He, F. Xu, F. Banhart, L. Sun, R.S. Ruoff, Spongy graphene as a highly efficient and recyclable sorbent for oils and organic solvents, Adv. Funct. Mater. 22 (2012) 4421-4425.

[38] C. Liu, J. Yang, Y. Tang, L. Yin, H. Tang, C. Li, Versatile fabrication of the magnetic polymer-based graphene foam and applications for oil–water separation, Colloids Surf. A 468 (2015) 10-16.

[39] C.-F. Wang, S.-J. Lin, Robust superhydrophobic/superoleophilic sponge for effective continuous absorption and expulsion of oil pollutants from water, ACS Appl. Mater. Interfaces 5 (2013) 8861-8864.

[40] L. Li, B. Li, L. Wu, X. Zhao, J. Zhang, Magnetic, superhydrophobic and durable silicone sponges and their applications in removal of organic pollutants from water, Chem. Commun.

50 (2014) 7831-7833.

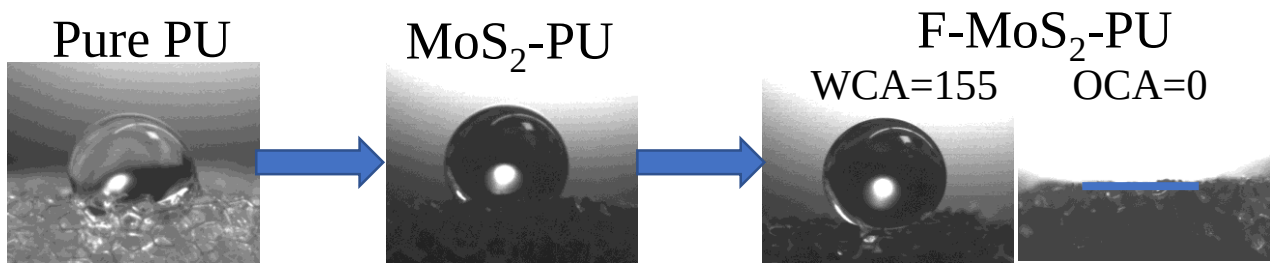

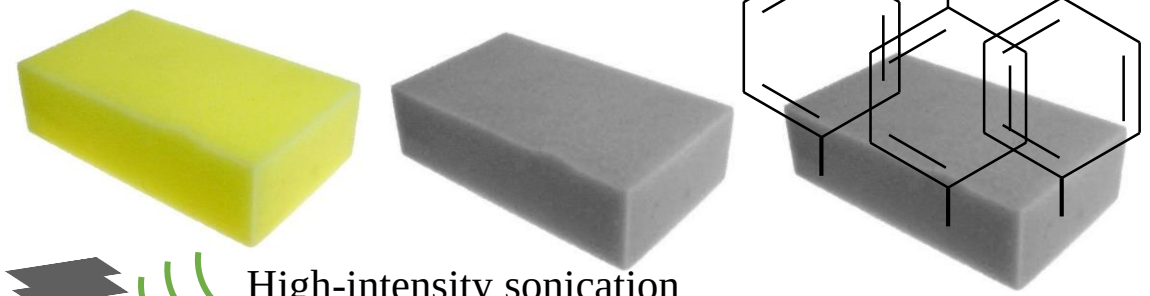

Demulsification

Underwater oil elimination

Oil/water separation

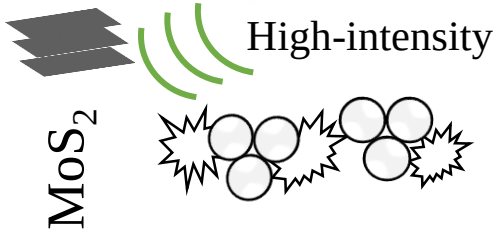

Explosion

Micro-jets

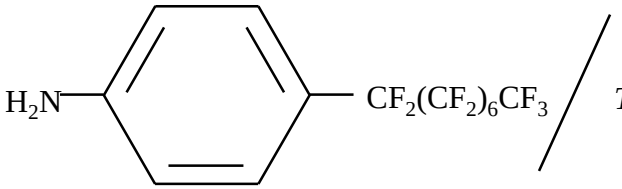

In situ functionalization

Before

After

PhMe/water